

1 Research Article – Attribution: CC-BY-ND.

2

3 **SARS-COV-2 THREE FORCING SEASONALITIES: POLICIES, ENVIRONMENT**  
4 **AND URBAN SPACES**

5 Charles Roberto Telles<sup>1</sup>

6 <sup>1</sup>Multisector Projects Division. Secretary of State for Education and Sport of Paraná. Água  
7 Verde Avenue, 2140. Água Verde. Curitiba - PR, 80240-900. Brazil.

8 Correspondence: [charlestelles@seed.pr.gov.br](mailto:charlestelles@seed.pr.gov.br)

9

10 **Abstract:** This research investigated if pandemic of SARS-COV-2 follows the Earth seasonality  $\varepsilon$   
11 comparing countries cumulative daily new infections incidence over Earth periodic time of  
12 interest for north and south hemisphere. It was found that no seasonality in this form  $\varepsilon$  occurs  
13 as far as a seasonality forcing behavior  $\varepsilon'$  assumes most of the influence in SARS-COV-2  
14 spreading patterns. Putting in order  $\varepsilon'$  of influence, there were identified three main forms of  
15 SARS-COV-2 of transmission behavior: during epidemics growth, policies are the main stronger  
16 seasonality forcing behavior of the epidemics followed by secondary and weaker  
17 environmental and urban spaces driving patterns of transmission. At outbreaks and control  
18 phase, environmental and urban spaces are the main seasonality forcing behavior due to  
19 policies/ALE limitations to address heterogeneity and confounding scenario of infection. Finally  
20 regarding S and R compartments of SIR model equations, control phases are the most reliable  
21 phase to predictive analysis.

22 These seasonality forcing behaviors cause environmental driven seasonality researches  
23 to face hidden or false observations due to policy/ALE interventions for each country and  
24 urban spaces characteristics. And also, it causes policies/ALE limitations to address urban  
25 spaces and environmental seasonality instabilities, thus generating posterior waves or  
26 uncontrolled patterns of transmission (fluctuations).

27 All this components affect the SARS-COV-2 spreading patterns simultaneously being  
28 not possible to observe environmental seasonality not associated intrinsically with policies/ALE  
29 and urban spaces, therefore conferring to these three forms of transmission spreading  
30 patterns, specific regions of analysis for time series data extraction.

31

32 **Keywords:** COVID-19; policies and ALE preventive methods; forced seasonality; Fourier  
33 transforms; environmental driven factors; urban spaces heterogeneity.

34

35 **1) Introduction**

36 The main focus of this research is to point, as noted in Grassly and Fraser [1], the  
37 consequences of seasonality for endemic  $R_0$  stability in order to understand and obtain an  
38 endemic equilibrium for COVID-19 involving mixing patterns such as environmental driving  
39 factors, policies interventions and urban spaces [3-8]. These three variables might pose a  
40 challenging outcome for predictive analysis [9] of SARS-COV-2 spreading patterns since the  
41 time series data of cumulative daily new cases are highly influenced by it in terms of  
42 quantitative outcomes day by day, fluctuations and mainly random outcomes that comes

NOTE: This preprint reports new research that has not been certified by peer review and should not be used to guide clinical practice.

43 influenced by different aspects of local epidemics behavior. In order to correct and address  
44 this later point, we might be observing data that should be divided in three phases of  
45 epidemics that is the outbreak, peak and control followed by its main seasonality drivers found  
46 in this research in sequence that is the environmental variables (Earth seasons and  
47 atmospheric conditions), policies and ALE interventions and urban spaces (local indoor and  
48 outdoor spaces for transit and social interactions being public or private with natural physical  
49 features on it). By observing time series data of cumulative daily new cases worldwide [10],  
50 these three sequences of epidemics phases present different results for each sample (country)  
51 of observation and many delays in order to obtain a normality for epidemic curve are found as  
52 well as attractive behavior of the outcomes over time. These constraints give the formation of  
53 false observations of phenomenon to predictive analysis based on SIR models and derivations  
54 [11], policies interventions and the main role of environmental variables towards outbreaks  
55 and waves restarting periods.

56 Following this late paragraph statements, this research divided the world data of  
57 cumulative daily new cases for COVID-19 in three regions of data extraction in the linear time  
58 series, designed to organize the confounding data of analysis, prediction and accuracy for  
59 fields of research. This will bring more robust understanding for the scientific convergence of  
60 results and worldwide strategies to reduce SARS-COV-2 spreading patterns of infection.

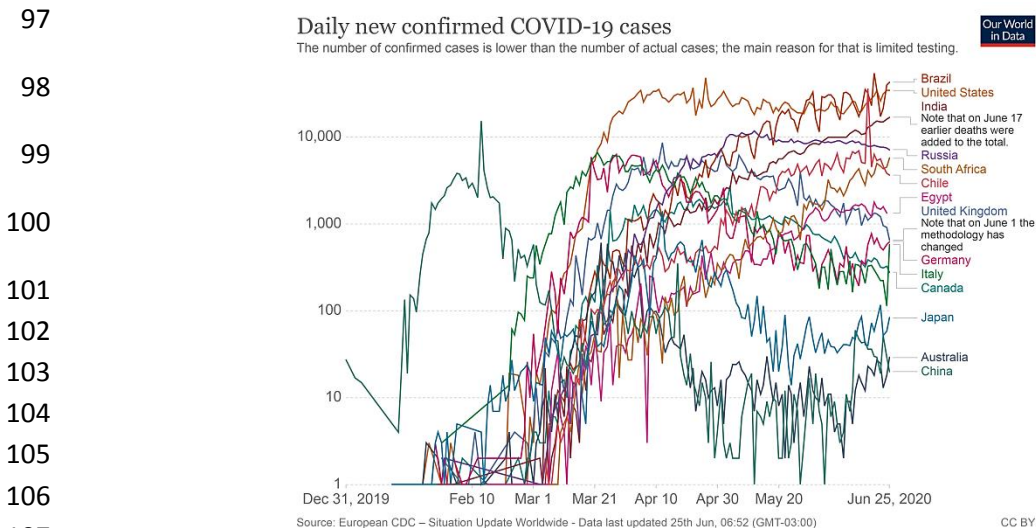
61

## 62 **2) Methodology**

### 63 2.1 Earth seasons: undefined time intervals of analysis for periodic oscillations

64 To put COVID-19 under the Earth seasons aspect of analysis the endemic free-  
65 equilibrium need to be under the view of Floquet Theory as it is current in many other  
66 infectious diseases with defined periodic  $T$  behavior (Earth seasonal ( $\varepsilon$ )) and we need to meet  
67 a periodic oscillation to predict  $R_0$  under  $A(t)$  criteria in time-varying environments with no  
68 heterogeneity forces, thus assuming a force of infection as  $F(T) = B(t) \frac{I}{N}$  in order to be  
69 possible to establish a reasonable  $R_0^T$  periodical stability for COVID-19 as observed by Bacaër  
70 [12] as defined in [12] as  $p(t+1) = (A(t) + B(t))p(t)$ , being  $p$  the spectral matrix and  $B(t)$   
71 the confounding environment (ecological variables such as biotic and abiotic) of compartments  
72 S, I and R of SIR model. At this point the seasonality of COVID-19 at S, I and R compartments is  
73 assumed to be dependent on deterministic outcomes for immunity, healthcare interventions  
74 and public policies under atmospheric triggering conditions (Earth seasons  $\varepsilon$ ) as found, for  
75 example, in common flu. If considering this condition, the ODE could be easily observed in  
76 linear time series as pointed in Sietto [13] as  $y(t) = a + bt + \sum_{i=1}^m c_i \cos\theta + \sum_{i=1}^m d_i \sin\theta +$   
77  $e(t)$ , where the proposition of periodicity  $\theta$  as linear in time as  $B(t+T) = B(t)$  would be  
78 possible and consistent in its fluctuations in terms of daily new infections with seasonal  
79 sinusoidal patterns as  $\theta(t) = \theta_0[1 \pm \varepsilon \sin(2\pi t)]$  [14], and also stochastic over time factor  
80 considering seasonal fluctuations defined as Hidden Markovians chains as  $P(Y(t) =$   
81  $y(t)|Y(t-1) = y(t-1), Y(t-2) = y(t-2), \dots, Y(1) = y(1))$  [13] and its many  
82 derivations, found in many researches, as examples [15-17], of the same event worldwide that  
83 would lead to the seasonal Fourier transform fluctuations of COVID-19 outbreaks and over  
84 defined time behavior. If each epidemics is universally assumed as equal towards  $\varepsilon$  worldwide,  
85 then Fourier analysis would be possible to be performed considering time periodic fluctuations  
86 as noted in Mari *et al* [14] and therefore, the use of Markovian chains to obtain the phase  
87 shifts of regularities would be a true approach to predict how SARS-COV-2 spreading patterns

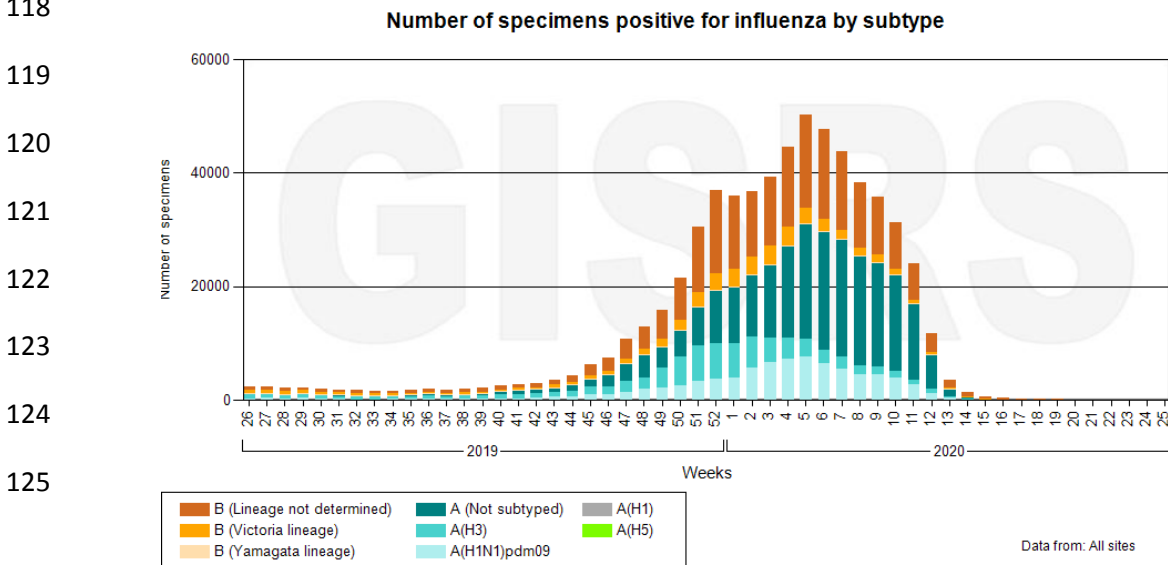
88 are formed. The main problem we face here is when the stochastic process  $Y(t)$  assumes a  
 89 lack of synchrony due to random delays [8,18,19] worldwide, hence generating a stochastic  
 90 form with unknown seasonality of infection as defined in [18] as  $R'_0 = D \int_0^1 B(t)dt$ , and  
 91 therefore, not assuming a seasonality for  $\varepsilon$  and the outbreak of local epidemics. At this point  
 92 we have several discrepant (heterogeneous) time series of the exponential behavior of daily  
 93 new cases infection in countries that were in winter season (figure 1) and also comparing  
 94 countries that are entering winter at south hemisphere and entering summer at north  
 95 hemisphere (figure 1). There is no strong difference between Earth seasonality influencing  
 96 those localities in its virus spreading patterns.



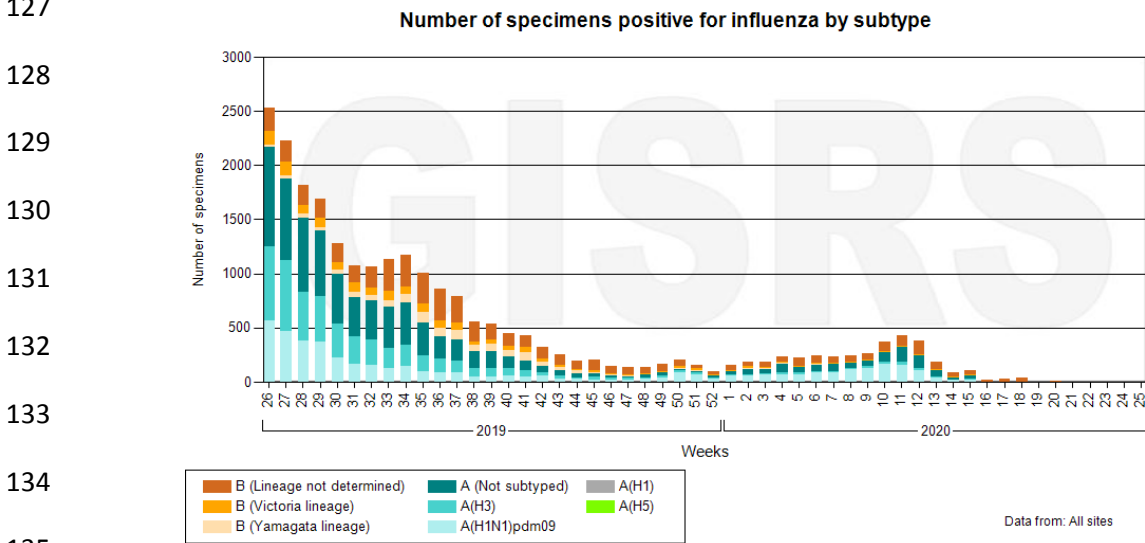
108 **Figure 1.** Selected countries from December 31, 2019 to June 25, 2020 from continents Asia, Europe, South and  
 109 North America, Africa and Australia were displayed interpolating Earth seasons and number of cumulative daily new  
 110 infections. Source: Our World in Data.

111

112 This lack of pattern formation as found in common flu [20] (figure 2 and 3) creates an  
 113 undefined  $T$  over defined  $A(t)$  as well as mean  $\mu$  (figure 2) over periodicity  $\theta$  criteria (figure 3)  
 114 as a pre assumption of analysis in the view of Fourier transform and therefore confirming an  
 115 unexpected seasonality forcing behavior  $\varepsilon'$  in which each sample (countries, regions, places,...)  
 116 presents a different SARS-COV-2 spreading pattern not only concerning the Earth seasonality,  
 117 but other components of  $\varepsilon'$  as presented in the introduction section.



126 **Figure 2.** Seasonality of Influenza common species by 2019 and 2020 at North Hemisphere. Source: WHO.  
 127



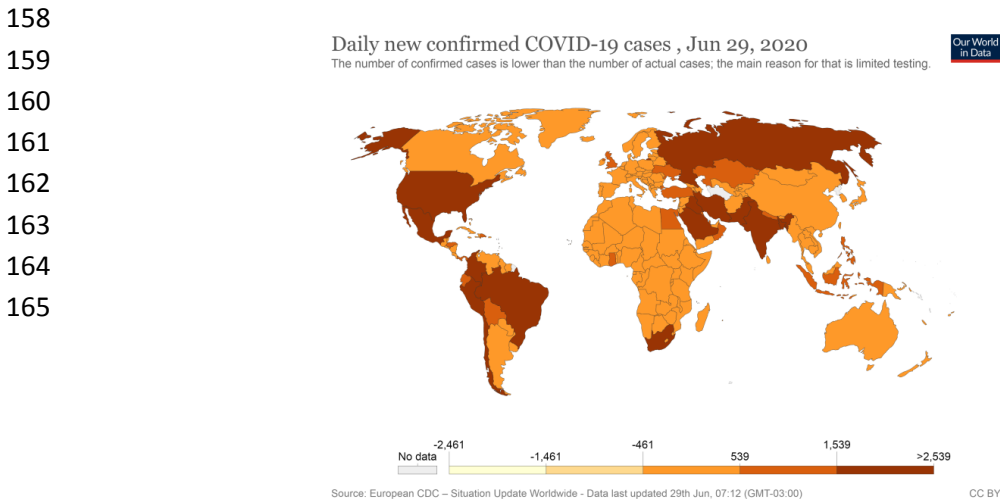
134 **Figure 3.** Seasonality of Influenza common species by 2019 and 2020 at South Hemisphere. Source: WHO.  
 135  
 136  
 137

138 **2.2 Seasonality forcing behavior beyond Earth seasons and sinusoidal approaches**

139 What we are observing clearly or maybe apparently at many results [2], is an  
 140 asymptotic unstable behavior of SARS-COV-2 towards atmospheric conditions dictated by  
 141 temperature, humidity, UV (ultraviolet) and wind speed as those results don't present  
 142 consistent indication of how atmospheric events have strong influence in the SARS-COV-2  
 143 spreading patterns of transmission as seasonal environmental drivers.

144 One might understand that north hemisphere had its first wave because of  
 145 atmospheric conditions such as Earth season periods and for that in its turn, the south  
 146 hemisphere as entering in winter will present exactly the same epidemics behavior presented  
 147 at the first wave impact as observed in north regions. One important observation over it refers  
 148 to the high amount of infection in north hemisphere in some countries under the summer  
 149 season in contrast to the same amount of infection in south hemisphere under winter season  
 150 that is occurring nowadays.

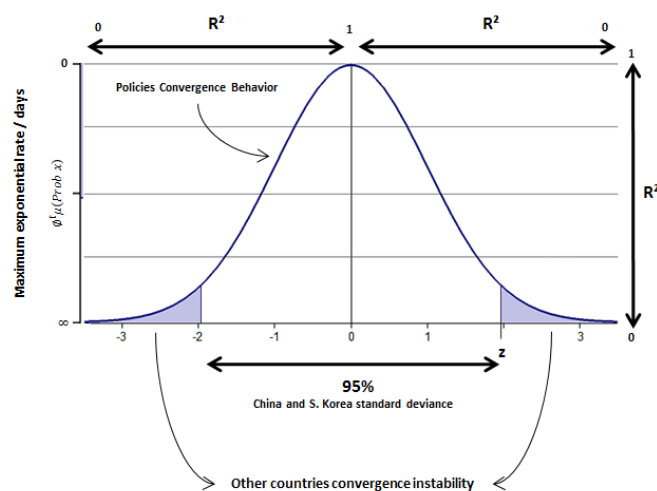
151 Both planet regions presented similar daily new infections at both seasons, therefore,  
 152 not differing in the transmission spreading patterns of infection. Following this path, no  
 153 periodic criterion was met for basic reproductive number  $R_0$  stability for an endemic  
 154 equilibrium. We are facing daily new cases worldwide (figure 4) and the reason for the north  
 155 hemisphere for European and Asian countries reduces its spreading patterns in the end of  
 156 winter season is rather a coincidence over time that was caused mainly due to policies and ALE  
 157 over population and individual behavior [3-8].



166 Figure 4: This graph mainly is focused in the comparison of north and south hemisphere countries such as Europe  
 167 that decreased epidemics due to policies intervention and south and North America countries that were hit by first  
 168 wave and policies were applied in different perspectives if compared to Europe. Source: Our World in Data.  
 169

170 If no seasonality of atmospheric conditions was found, we can observe still a  
 171 seasonality forcing behavior, which was very well shaped by contact rates frameworks [4]  
 172 based on policies and ALE actions [6] as represented in Figure 5. Bell shaped curve scheme.  
 173 This overall scenario of pandemics could be very well observed in late March and starting April  
 174 when at that time China and South Korea were the countries with the most lower rates of  
 175 exponential growth of infection while Europe was in its growing pattern fully active and also in  
 176 later June, many other researches pointed to the importance and role of policies and ALE  
 177 towards pandemic control rather than atmospheric patterns of infection spreading worldwide  
 178 [2-9].

179  
 180  
 181  
 182  
 183  
 184  
 185  
 186  
 187  
 188  
 189  
 190  
 191



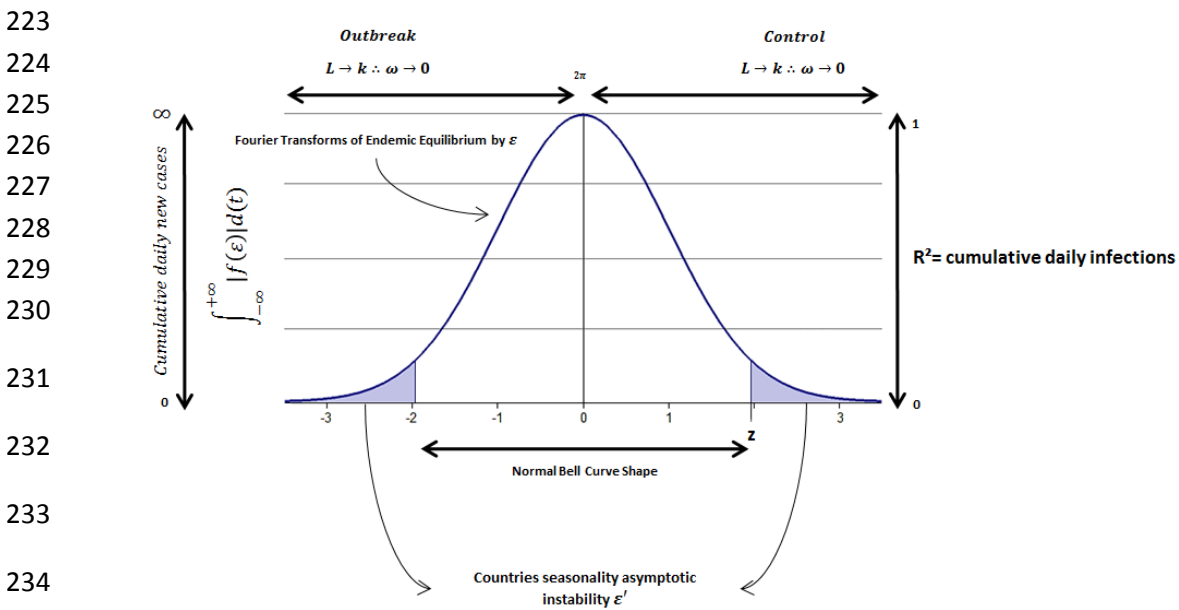
192 Figure 5: China and South Korea policies intervention effect over COVID-19 spreading pattern in late March and  
 193 April, followed by other countries patterns. This was proved to be true [2-8] over time of pandemic outbreak  
 194 regarding policies and SARS-COV-2 spreading patterns data.  
 195

196 But it does not mean that environmental variables such as atmosphere properties or  
 197 Earth seasonality present no causation on the event (this will not be demonstrated and it is  
 198 only theoretically assumed for the long-term expression of the pandemics, of which we don't  
 199 have still a visible glance of it). It means exactly that policies and ALE influence the  
 200 phenomenon in different degree of seasonal forcing behavior than was expected to be  
 201 addressed to the environmental factors, since we already have these outcomes available in  
 202 worldwide data.

203 And also, not mentioned yet, the urban spaces found in every city, present specific  
 204 potential to influence the local epidemics for the S and R compartments of SIR models, since it  
 205 affects the capability of each country/city/locality to deal with the outcomes of susceptibility,  
 206 immunity and public health control measures, therefore, making COVID-19 predictive models  
 207 to assume data that are not perfectly real. And for each predictive model that fails to address  
 208 urban spaces heterogeneity, policies and ALE interventions subjectivity and environmental  
 209 non-homology of data, uncertainty degree grows making SARS-COV-2 emerge under unknown  
 210 patterns of contagion as observed in Billings et al [19] and with a similar example of measles in  
 211 Grenfell et al [21].

212 2.2 Seasonality forcing behavior

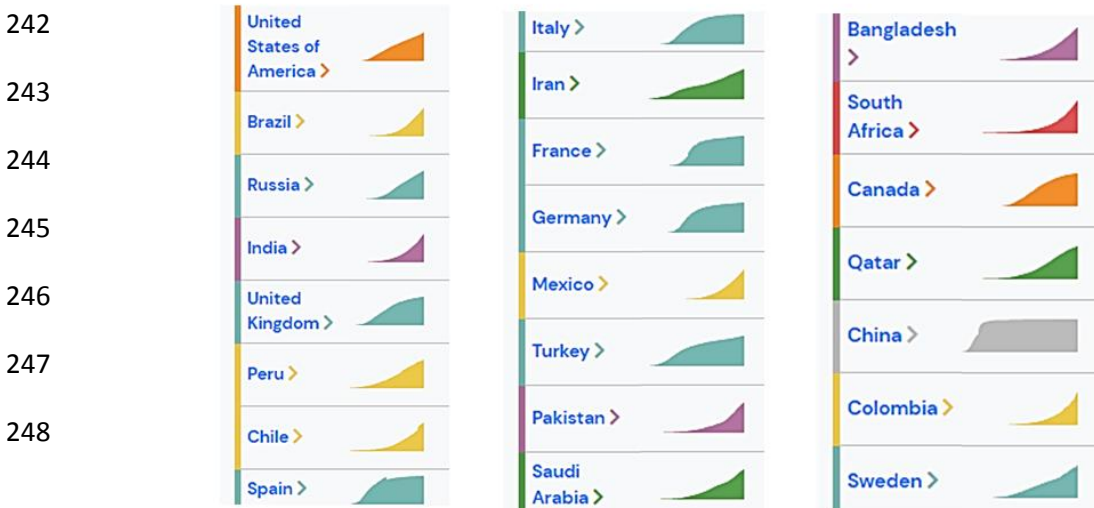
213 The unexpected seasonality under heterogeneity forcing behavior  $\varepsilon'$  might confer to  
 214 the exponential behavior of infection spreading patterns among countries an unpredictable  
 215 sinusoidal expression like  $\beta(t) = \beta_0(1 + \varepsilon\phi(t))$  as pointed by Buonomo et al [22] of Fourier  
 216 transforms considering finite time lengths of analysis (seasons) equally distributed over time  
 217 period  $T$  within samples (countries). This can be better understood because of the data series  
 218 of cumulative daily new cases present high-amplitude noise and this is often related to the  
 219 lower spectral density and lower frequency in which makes the analysis imprecise as a  
 220 sinusoidal behavior in the basis form of Earth seasonality as  $\int_{-\infty}^{+\infty} |f(\varepsilon)|d(t)$ . In this sense, the  
 221 sinusoidal behavior does not exist in terms of how countries might present default oscillations  
 222 within seasonal periods of Earth as represented schematically in figure 6.



235 **Figure 6.** General framework of covid-19 seasonality under the view of Fourier transforms limitations.

236

237 And following this path, this leads to the observation that each sample can be  
 238 understood as the lack of forming patterns towards confident interval and standard deviation  
 239 under default time periods  $T$  from December 31, 2019 to June 25, 2020, resulting into a  
 240 stochastic maximum exponential form of cumulative daily new infections as  $Y(t)$  change over  
 241 time as showed in figure 7 samples.



249 **Figure 7.** Some countries spreading patterns since outbreaks until June 25, 2020. Source: Outbreak.info.

250

251 However, despite of this scheme pointing to the weaker Earth seasonality forcing  
252 behavior of SARS-COV-2 spreading patterns, they can still be influencing the overall pattern of  
253 transmission with a hidden pattern due to policies/ALE interventions, environmental driven  
254 seasonality and urban spaces.

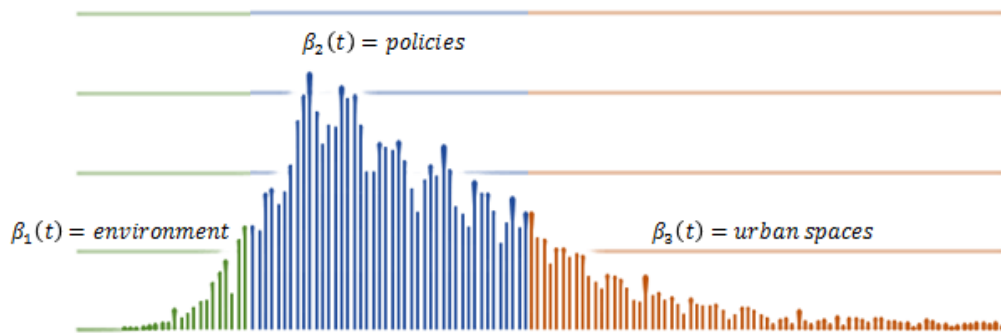
255 This point can be addressed to the pattern formation of  $\varepsilon'$  confounding forced seasonality  
256 for S and R compartments over time [1,23-29], environmental driven factors [30-32] and  
257 policies/ALE intervention [3-8]. It is possible to observe (figure 1, 3 and 7) that each country  
258 dimension might respond differently to the same initial conditions, influenced by these three  
259 components, thus generating multiple patterns formation over time  $T$  for SARS-COV-2  
260 transmission and periodicity.

261 Concerning a theoretical desired worldwide normal distribution that most mathematical  
262 models implies for infection spreading patterns with shape behavior  $k = 1$  or  $k > 1$  (Weinbull  
263 parameterization) of exponential "irregular" distributions of SARS-CoV-2 infection within time  
264 intervals  $t$  with defined periodicity  $T$  (seasonality among countries) [33], the defined original  
265 form of  $I$  compartment is given as  $\frac{dI}{dt} = \beta \frac{SI}{N} - gI$ . However, the high asymptotic instability  
266 behavior [23-29] of  $I$  lead us to redefine the equation basic fundamentals and it can be  
267 understood as  $I = \left(\frac{\omega}{\lambda}\right)^k (1)$ , where the infected  $I$  is influenced by unpredictable scale of  
268 infection  $\lambda (N)$  with inconsistent behavior of variables transition rate ( $\beta SI$ ) defined as  $\omega$ , and is  
269 not assumed for  $gI$  in the original form of R, that there are a normal distribution output for  
270 this virus spreading patterns. This new pattern formation of the epidemic behavior was well  
271 pointed by Duarte et al [34] when contact rate do not take in account weather conditions and  
272 time-varying aspects of epidemics. Therefore it was used an unpredictable shape  $k$  (close to  
273 reality shapes), mainly defining this shape caused  $\lambda$  and  $\omega$  asymptotic instabilities generated  
274 by S and R compartments over time [1,23-29], environmental driven factors [30-32] and  
275 policies/ALE intervention [3-8]. This equation represents the presence of confounding and  
276 heterogeneous environmental variables  $\omega$  with unknown predictive scale of  $exp \lambda$  or  
277 maximum likelihood estimator for  $\lambda$  due to nonlinear inputs for S and R (urban spaces), policies  
278 and environmental conditions influence, and therefore generating nonlinear outputs  $k$   
279 (asymptotic instability) [35,36]. If we consider that most models are searching for a normality  
280 behavior among countries, hence, implying that the  $k$  distributions are non-complex and not  
281 segmented by its partitions, therefore resulting into a linearity for the virus infection  $I$  over  
282  $Y(t)$  and  $t$ , then the overall equation as described by Dietz  $\beta(t) = \beta m(1 + A \cos(\omega t))$  [35]  
283 would be not reachable for any given time period of analysis considering the seasonality  
284 forcing behavior of SARS-CoV-2.

285 The outputs with heteroscedasticity and non-homologous form for  $k$  and  $\lambda$  can be  
286 modified to reach stable points of analysis in as modeled by Dietz  $\beta(t) = \beta m(1 + A \cos(\omega t))$   
287 for each of the three seasonality forces influencing SARS-CoV-2 spreading patterns, that is  
288 regions where Fourier transforms and other methods of predictive analysis based on SIR  
289 models and derivations, policies interventions and the main role of environmental variables  
290 towards outbreaks and waves restarting periods can be found. These stable points of  
291 asymptotic convergence can be observed in the scheme of figure 8.

292

293  
294  
295  
296  
297  
298  
299  
300  
301



302  
303  
304  
305  
306  
307

Figure 8. Concerning the apparent exclusion of Earth well defined seasonality, the external forcing behavior of SARS-COV-2 spreading patterns can be now filtered and stated as presenting three phases of expression, that is the S and R compartments constraints to modeling aspects, environmental driven and confounding variables and policies/ALE interventions conferring to the modeling aspects of prediction, undesirable uncertainty degree not only for outbreaks, second waves.

308  
309  
310  
311

In order to remove heteroscedasticity and non-homologous form for  $k$  and  $\lambda$  from occurring, as far as the  $\kappa < 1$  Weibull parameterization aspect [37] (Bell curve shape) of distribution be elected as the most reliable region of analysis (attractive orientation) for any given  $T$  periods within samples (countries cumulative daily new cases time series), it is

312  
313  
314  
315  
316  
317  
318

necessary to modify the first equation (1) to  $I = \left(\frac{Y(t)}{T}\right)^{\pi < y < \frac{\pi}{2}} - \left(\frac{\omega}{\lambda}\right)^k$  (2), hence with the new SIR model proposition as  $I = I' - S + R$ , where  $I$  is asymptotic to  $I'$  and S and R considered in its original form  $\theta(t) = \theta_0[1 \pm \varepsilon \sin(2\pi t)]$  [14]. This is a mandatory redesign since many scientific breakthroughs are pointing to policies as the best approaches to reduce COVID-19 nowadays [3-8]. Starting with this redesign of equation we might find one of the first region of analysis and stability, which is policies intervention, found in the slope (peak) of daily cumulative cases over time.

319  
320  
321  
322  
323  
324

Let's address this persistence homology briefly for this research, where this desired mean function  $Y(t)$  of topological space  $\mathbb{X} \rightarrow \mathbb{R}$  over  $\beta(t) = \beta m(1 + A \cos(\omega t))$  indicated at (2) can be found as a persistence diagram existence [38] by mapping each adjacent pair to the point  $(f(Y(t)), f(t))$  minimum and maximum observations, resulting in critical points of  $Y(t)$  function over time  $t$  not in adjacent form globally but regionally triangularly space as  $d(D(Y_t), D(t)) \leq \|Y_t - t\|_\infty$  [39] with a given mean region, thus expressing random critical

325  
326  
327  
328  
329  
330  
331

values defined by  $I = \left(\frac{\omega}{\lambda}\right)^k$  in the original form of observation of the event. But since we need to filter  $f(Y(t)) - f(t)$  unstable critical points (oscillatory instability of seasonality for S and R policies/ALE and environmental driven variables) to an attractive minimum behavior with normal distribution, then this region of analysis must be situated between  $\pi < Y(t), t < \frac{\pi}{2}$  for every  $A(t) \rightarrow T$  asymptote periods. Following this path, we going to have a roughly speaking the mean as the size of persistence diagram and triangulable diagonal ( $\Delta$ ) like  $D(Y_t, t - \Delta) = \sum_{\pi < Y(t) < \frac{\pi}{2}} \mu_t^{Y_t}$  with multiplicity pairing regions  $(t, Y_t)$  for each desired triangulation as

332  
333  
334  
335

$0 \leq t < Y_t \leq n + 1$ , resulting in the general equation for any assumed region as  $\mu_t^{Y_t} = \beta(t)_{\varepsilon_{t-1}}^{\varepsilon_{Y_t}} - \beta(t)_{\varepsilon_t}^{\varepsilon_{Y_t}} + \beta(t)_{\varepsilon_t}^{\varepsilon_{Y_t-1}} - \beta(t)_{\varepsilon_{t-1}}^{\varepsilon_{Y_t-1}}$  [39]. Note that each mean function  $\mu_t^{Y_t}$  will be given by regions defined as  $\beta(t) = \beta m(1 + A \cos(\omega t))$ , being  $\beta(t)$  the covariance function of seasonality forcing behavior  $\mu(A(t))$ , therefore without a global mean value for the event in

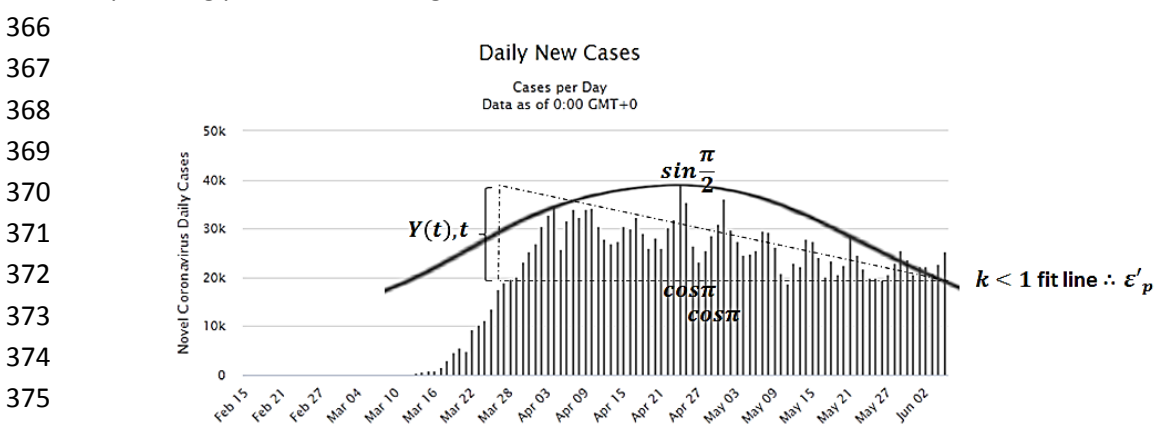


336 terms of infection and time. Further derivations and formulations regarding this persistence  
 337 diagram won't be addressed for this research, but it is highly suggested that future researches  
 338 keep these formulation defined for predictive and monitoring analysis of epidemic seasonality  
 339 forcing behavior.

340 Also, it is necessary to understand that this new design of seasonality regions can be  
 341 properly adapted to Fourier transform analysis under the amplitude of waves with the  
 342 equation  $e^{-i\omega t} = \cos(2\pi t) + i \sin(2\pi t)$  where angular momentum was drawn in the limits of  
 343  $\beta(t) = \beta m(1 + A \cos(\omega t))$ , giving  $\omega = \pi < Y(t), t < \frac{\pi}{2}$  and generally defining it with sinusoidal  
 344 reduced form as  $f(\epsilon') = \int_{-\infty}^{+\infty} Y(t) e^{-2\pi i \omega t} d\omega$  in order to reach a sinusoidal approach of time  
 345 series data extraction and analysis over time periods and regions of analysis.

346 Also beyond the limitation of time periods for predictive analysis and monitoring as a  
 347 Gaussian Process, this design also introduces one main point of analysis that is the lack of a  
 348 mean and covariance function  $\mu(Y(t))$  over fluctuations as a global homomorphism and a  
 349 decomposition form of wave signals similar to Fourier transforms where persistent homology  
 350 can be found for  $t \therefore \kappa < 1$  Weibull reliability to be situated in the oscillations pairing region of  
 351  $\sin(\pi) = 1$  and  $\cos(\pi) = 0$  for  $T$  desired coordinates of fluctuations in  $(f(Y_t), f(t))$  of  
 352 stability with  $t + 1$  continuous form as  $\delta = f(Y_t, t) \int_{\frac{\pi}{2}}^{\pi} \mu \sum(Y_0, \dots, Y_n) d\mu$  [9], thus assuming the  
 353 shape and limit to  $\kappa < 1$  as small partitions to the desired analysis or without a derivative form  
 354 for the overall analysis within the period defined. For the discretized view of  $Y_t, t$  as pointed in  
 355 [9] results, it is possible to obtain a sample mean as  $\bar{\mu} = \frac{1}{n} \sum_i^n Y_t, t$ . Further results of this  
 356 approach can be visualized at [9] reference.

357 At this point, by rejecting the persistence diagram unstable critical points generated, a  
 358 local minimum of the event as an average mean can be obtained by having  $Y(t)$  with the  
 359 higher number of samples  $Y$  (daily infections) that finds a condition roughly described in the  
 360 nonlinear oscillations within the exponential growth epidemic behavior of event as limited  
 361 between local maximum growth defined by  $\frac{\pi}{2}$  by its half curvature oscillations  $\pi$  as a local  
 362 minimum being non periodic as  $2\pi$  in a global homomorphism sense due to  $\kappa < 1$ . In this  
 363 sense, the new sinusoidal approach offers new mean function as an angular momentum of  
 364  $\omega = \pi < Y(t), t < \frac{\pi}{2}$ . This scheme can be observed for policies/ALE intervention on SARS-CoV-2  
 365 spreading patterns [23] in figure 9.



377 Figure 9. Policies/ALE stable region of analysis on SARS-CoV-2 spreading patterns. Image data source: Worldometer  
 378 – Italy on 08 July 2020.

379

380 Therefore  $Y(t), t$  assumes the desired oscillations samples and region condition like  
 381  $\pi < Y(t), t < \frac{\pi}{2}$  where persistent homology can be found for  $t \therefore \kappa < 1$  to be situated in the  
 382 oscillations pairing region of  $\sin(\pi) = 0$  and  $\cos(\pi) = Y(t)$  for  $Y(t), t$  desired coordinates  
 383  $(f(Y(t)), f(t))$  of stability with  $t + 1$  as  $Y(t) = f(Y(t)) \int_{\frac{\pi}{2}}^{\pi} \mu \sum(Y_0, \dots, Y_n) dt$  or vice-versa for  
 384  $t = f(t) \int_{\frac{\pi}{2}}^{\pi} \mu \sum(t_0, \dots, t_n) dY_t$ , thus assuming the shape and limit to  $\kappa < 1$ . Then concerning  
 385 time lengths of samples, it is designed as  $t(\delta + 1) \leq f(Y(t)) \mu \sum(Y_0, \dots, Y_n) dt$  starting from  
 386  $t_0, \dots, t_n \leq \sin(\frac{\pi}{2})$  results in the desired data distribution with a conditional shape of Weibull  
 387 parameterization  $\kappa < 1$  for the analysis with a normal distribution, therefore rejecting any  
 388 critical value beyond  $\cos(\pi) = \varepsilon'_p$  and under  $\sin(\pi) = \varepsilon'_p$ , being  $\varepsilon'_p$  the seasonality forcing  
 389 behavior of policies intervention over SARS-CoV-2 among countries data sets.

390 Now, considering that the S and R compartments of SIR model are needed to  
 391 predictive analysis of infection spreading patterns, these compartments might work properly  
 392 under the third region of time series data, that is the urban spaces  $\varepsilon'_u$  seasonality. To achieve  
 393 these results with high reduction of uncertainty, it is necessary to conceive S and R as in its  
 394 most stable region of analysis, that should be influenced in a posterior scenario where  $\varepsilon'_p$   
 395 (policies/ALE) and  $\varepsilon'_e$  (environmental seasonality) already took effect. This is mandatory since  
 396 as far as policies are assumed in models or estimated with unreal quantitative parameters they  
 397 promote uncertainty growth, and also they face limitations to track real patterns within an  
 398 urban space features for S and R as a causation relation. For urban spaces seasonality forcing  
 399 behavior, it is considered that inside and outside spaces promotes limitations to policies/ALE  
 400 due to limiting action that it can face within these urban spaces (not all policies/ALE can  
 401 survive in some urban spaces as it was designed to be). And also environmental seasonality  
 402 can be present at this phase influencing with urban spaces the limitation of policies/ALE  
 403 actions, therefore,  $\varepsilon'_e$  might find a spot to grow within inside and outside urban spaces  
 404 beyond  $\varepsilon'_p$  normalization (more explanation of this causation effect will be given in results  
 405 section).

406 Considering unexpected seasonal forcing  $\varepsilon'_p$  roughly defined as  $\partial(t) = \partial_0[1 \pm$   
 407  $\varepsilon_0 \cos \pi < \varepsilon' < \sin \frac{\pi}{2}]$  [9] in a complex network model, where non periodic oscillation  
 408 (sinusoidal) are to be found in discrete form with  $f(\varepsilon'_{e,p,u}) = \int_{-\infty}^{+\infty} Y(t), te^{-2\pi i \omega t} d\omega$ , we might  
 409 assume a rupture of the  $\sin(2\pi t)$ , leaving the region the pre assumed linearity  $\theta(t) = \theta_0[1 \pm$   
 410  $\varepsilon \sin(2\pi t)]$  for S and R in the overall metrics of time series data  $T$  within one sample or among  
 411 countries and understand each iteration of the event as unconnected to the previous and  
 412 future data if considering multiple time series comparisons (among countries) or even in the  
 413 same time series if considering long-term analysis. In true, since the  $I'$  is asymptote to  $\varepsilon'_p$ ,  
 414 then  $\varepsilon'_u$  is limited by  $\varepsilon'_p$  on  $I'$ , but not necessarily fully stable in terms of  $\varepsilon'_p$  present total  
 415 control over environmental seasonality due to urban spaces features. This statement is  
 416 understood as far as policies/ALE interventions are the strongest attractive point of the  
 417 phenomenon and therefore, compartment models find its limitation over how policies are  
 418 implemented and how urban spaces can be convergent to policies/ALE interventions. Is is  
 419 possible to check that most of these SIR models are constructed based on these  $\varepsilon'_p$  seasonality  
 420 behaviors [40]. From this phase on, urban spaces and policies/ALE interventions might present  
 421 high influence on the outcomes due to unpredictability of S and R patterns to design

422 appropriate contact rate and that is still a limitation for the SIR model methods nowadays [23-  
423 29], however, it is still the most desirable region of analysis for data extraction.

424 Concerning urban spaces, due to huge diversity of public health infrastructure buildings  
425 design, outdoor and indoor building designs and natural physical features such as rivers, lakes,  
426 snow,..., it influences the environmental driven pattern on the region and not only policies.  
427 Therefore, it is reasonable to understand that any assumption on S and R during epidemic  
428 phase in its full curvature is much more closed to uncertainty measures than ever.

429 In this sense, countries might diverge seriously in the urban space and therefore, and S  
430 and R compartments finds limitations to calculate it during peak curvature and also it is  
431 contradictory since policies are not even fully developed or had the time to take effect while  
432 these models uses policies as the basis of modeling patterns. For this reason, the most reliable  
433 region of analysis for these compartments and where most of the models are  
434 situated/functioning actually, remains at the control phase of epidemics, that is when  
435 exponential behavior reaches asymptotic stability towards SARS-CoV-2 reduction, and of  
436 course, caused by policies interventions mostly. However, fluctuations still may occur  
437 worldwide due to the type of policy/ALE features and urban spaces features. In sense, no  
438 perfect prediction can be achieved still, but it is the most stable region for predictive analysis.

439 Now let's assume that uncontrolled environmental driven factors  $\varepsilon'_e$  are the main cause  
440 of outbreaks and posterior waves of infection in a coupling relation with urban spaces and  
441 policies/ALE limitations, with unknown spreading pattern. This assumption can be confirmed  
442 since at this phase for the initial outbreak among countries, no policies intervention was  
443 existent or ALE features vary a lot among countries and also, as far as countries relax their  
444 policies [4,6,8], policies present urban spaces limitations and urban spaces promotes  
445 environmental seasonality, new waves of infection occur. In this sense, the environmental  
446 seasonality drivers as the main cause of aperiodic and unstable behavior for SARS-COV-2  
447 spreading patterns worldwide.

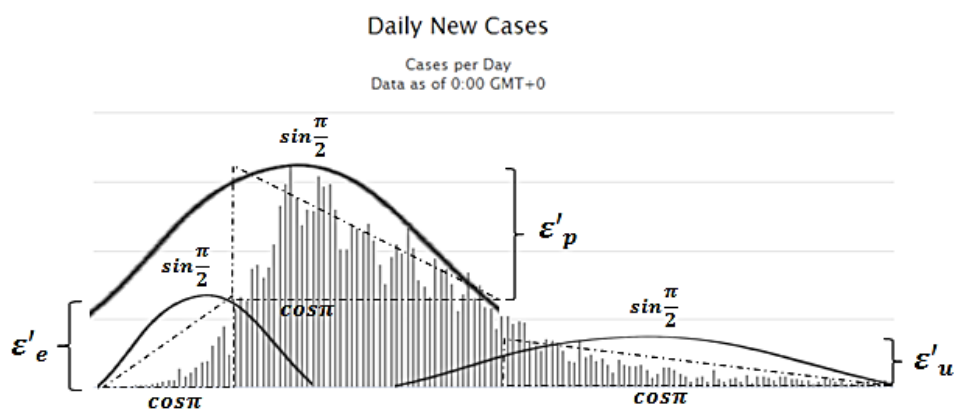
448 Extracting the patterns of transmission of SARS-COV-2 at this point is challenging in  
449 terms of identify how outbreaks and positive control of epidemics occurs. It is possible to  
450 address to the outbreaks the main cause of environmental drivers of seasonality for SARS-  
451 COV-2 when we understand that no policies/distinct ALE are influencing the phenomenon at  
452 this phase. And also at this point of analysis, second or other waves of infection have its main  
453 focus for researchers since that, as outbreaks, waves can be very closed related to the  
454 environmental variables and urban spaces rather than any other form of seasonality forcing  
455 behavior.

456 The uncertainty growth of epidemics patterns worldwide within the outbreaks need to  
457 be understood excluding the policies intervention region of analysis, since this region present a  
458 stronger seasonality forcing behavior for SARS-COV-2 and therefore at this point, the  
459 environmental drivers and urban spaces will be hidden on its potential to influence the disease  
460 dynamics. Following this statement, the most reliable region to investigate environmental  
461 seasonality remains at the outbreak and control phases while urban space seasonality remain  
462 at control phase. This can be very useful for policies and ALE approaches since the  
463 fluctuations/instability present at this region is caused mainly by these two forcing behaviors  
464 and therefore, new strategies and measurements need to be adopted in order to keep  
465 economy and prevention with similar power.

466 It was observed lately that China presented a second wave of infection, as far as, it  
 467 reduced some types of policies intervention, and therefore, it presented the urban spaces and  
 468 environmental driving factor for SARS-COV-2 spreading patterns, being it the remaining  
 469 infected citizens, environmental active virus, urban spaces outside scope of adopted policies or  
 470 even the atmospheric influence for the disease transmission in any of these variables such as  
 471 humidity, temperature, aerosols, wind, UV, etc.

472 If we could be capable of analyzing the outbreaks for first or second waves, we could  
 473 be able to understand how SARS-COV-2 is influenced by urban and environmental seasonality  
 474 comparing each country or region/locality with specific patterns for the environmental and  
 475 urban variables. In this point, this research addresses new reformulations of urban and  
 476 environmental variables influence and COVID-19 data sets under the view of cause and effect  
 477 in the specific outbreaks region of analysis as showed in figure 10.

478  
 479  
 480



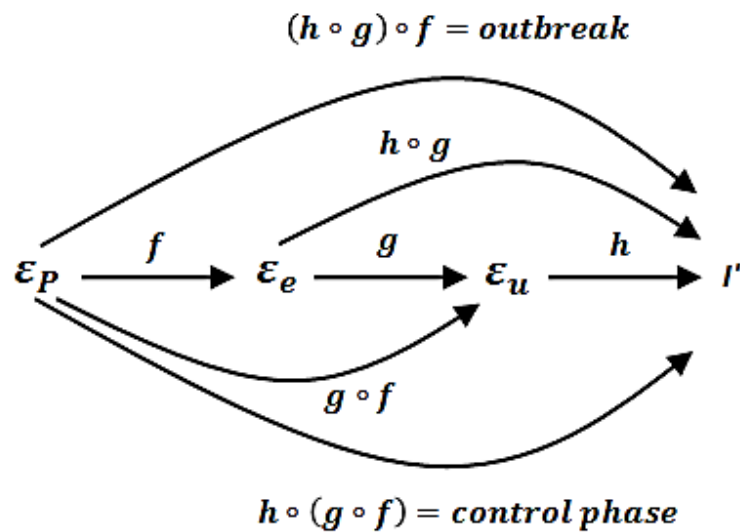
481  
 482  
 483  
 484  
 485  
 486  
 487  
 488

489 Figure 9. Considering the observation of figure 10, it is showed the asymptotic strong seasonality force of  
 490 policies/ALE ( $\varepsilon'_p$ ) intervention and the narrow and instable region (outbreak and control) of analysis for  
 491 environmental and urban driving factors of seasonality ( $\varepsilon'_e$ ,  $\varepsilon'_u$ ). Also regarding compartments S and R, the phase  
 492 where control is reached by policies intervention remain as the most stable region of analysis for this SIR model  
 493 equation compartments despite of instabilities cause by  $\varepsilon'_e$  and  $\varepsilon'_u$ .  
 494

### 495 3) Results

496 The overall scenario of transmission and spreading patterns can be visualized by the  
 497 scheme of figure 10, where seasonality forcing behavior assumes the following topological  
 498 spaces. Considering all the possible seasonality types,  $f(\varepsilon'_{e,p,u}) = \int_{-\infty}^{+\infty} Y(t) \cdot te^{-2\pi i\omega t} d\omega$ , in  
 499 continuous form of observation, and therefore, needing to be discretized within causal roots of  
 500 analysis due to heterogeneity and confounding environment of analysis, therefore, each  
 501 seasonality form can be understood as  $f\varepsilon'_p = g \circ f(Y_t, t) = g(f(\varepsilon'_p))$ , hence it can be also  
 502 wrote as,  $f\varepsilon'_p = h \circ (g \circ f(Y_t, t)) = h(g(f(\varepsilon'_p)))$  as a control phase of local epidemics.  
 503 However, this phase might present high instability (fluctuations) worldwide due to  
 504 heterogeneity and confounding behavior of  $f\varepsilon'_u$  and  $f\varepsilon'_e$ . And since, SIR models need stable  
 505 points for S and R, therefore  $f\varepsilon'_u = h \circ g(Y_t, t) = h(g(\varepsilon'_u))$ , resulting into a stable  
 506 asymptotic convergence only if  $f\varepsilon'_p = h \circ (g \circ f(Y_t, t)) = h(g(f(\varepsilon'_p)))$ . And since the  
 507 outbreak might find unknown patterns for  $f\varepsilon'_p$ ,  $f\varepsilon'_e$  and  $f\varepsilon'_u$ , then this region need to be  
 508 carefully considered, and therefore environmental seasonality can be found as  $f\varepsilon'_e = (h \circ$

509  $g(Y_t, t) \circ f = f(h(g(\varepsilon'_e)))$  or it is also possible to assume  $f\varepsilon'_e = (\varepsilon \circ g(Y_t, t))$ , being  $\varepsilon$  the  
 510 undefined patterns of environmental driven new infections for Earth seasonality or  
 511 atmospheric factors.



527 Figure 10. Schematically represented, the seasonality forcing behavior might assume the following behaviors:  
 528 during the local epidemics, environment and urban spaces can be defined by policies/ALE until a limit;  
 529 compartmental models are influenced by policies/ALE, environment and urban spaces; at control phase,  
 530 policies/ALE finds its limitation by environment and urban spaces and finally, at outbreak, environmental factors  
 531 present outcomes caused by the existing policies/ALE and urban spaces.

532

533 Note that there are a great different between environment driven seasonality being  
 534 caused by urban spaces influenced by policies/ALE limitations or otherwise caused by Earth or  
 535 other natural (atmospheric) seasonality forcing behavior at outbreaks. This should be carefully  
 536 considered when investigating Earth seasonality among countries. The compartmental models  
 537 are mostly in the control phase region and they lose efficacy at outbreaks where no specific  
 538 parameters are given and environmental seasonality is not yet discovered in its true patterns.  
 539 Also, compartments models present high uncertainty during policies/ALE interventions phase  
 540 and they work properly with empirical adopted policies (control phase) rather than pre  
 541 assumed theoretical simulations. Another points is regarding control phase where instabilities  
 542 occur as far as urban spaces creates a scenario where policies/ALE face limitations and  
 543 therefore, environmental seasonality find suitable place to grow in its patterns.

544 Due to uncertainty growth over time and the lack of mean for defined intervals of  $t$   
 545 over  $T$  normal distribution shape for the whole data, Earth seasons  $\varepsilon$  loses its effect gradually  
 546 as can be seen in figure 9 and 10 and the random delays observed for each country of analysis  
 547 (sample) can be attributed by different patterns in which outbreak occurs since existing  
 548 policies/ALE are found within world cultures, science and education. Earth seasonality should,  
 549 for now, be addressed in terms of how it can influence transmission rather than seasonality  
 550 patterns due to very limited overview of the event over time.

551 Also assuming the last researches on the field [3-8], policies and ALE are the most  
 552 strong seasonality force influence the behavior of epidemics at second and third phase of time  
 553 series data, while environmental factors are hidden in terms of transmission power at  
 554 outbreaks and control phase giving unobserved and possible wrong results concerning this

555 type of research. Another point of environmental convergence to SARS-COV-2 spreading  
556 patterns remains in the inside and outside of urban spaces where variables assume nonlinear  
557 forms of inputs and outputs and confounding outcomes with policies/ALE limitations, thus  
558 misleading the true behavior of infection spreading patterns under atmospheric parameters  
559 analysis (environmental seasonality). In this sense, it is very possible that environmental driven  
560 seasonality results found in many researches are in true, policies/ALE and urban spaces results.  
561 More detailed research need to be conducted. Inside and outside urban spaces are very  
562 important variables that can drive environmental research during all epidemics and concerning  
563 policies/ALE at the control phase and finally, possibly influencing with high uncertainty the  
564 compartment models for the susceptible and removed. For environmental seasonality  
565 evidences and complete description of atmospheric events influencing SARS-COV-2  
566 transmission an artificial environment would be the best initial approach to reach that  
567 discover. This is because in the natural environment, the confounding variables involving  
568 transmission, presented as three phases in this research, can hide the true patterns of  
569 transmission considering UV, humidity, wind, temperature and other factors.

570 Therefore, having policies and ALE as the most convergent and stable interaction with  
571 the SARS-COV-2 spreading patterns, environmental and urban factors are presented as  
572 secondary influence which makes difficult for outside analysis to perform confident measures  
573 of its influencing power. The same happens for SIR models predictive analysis when it  
574 considers worldwide equal adopted policies or no environmental influence for the outbreak or  
575 control phases. Though secondary, it assumes a major importance at control phase, since it is  
576 the main cause of policies/ALE limitations to reduce or even end the transmission complex  
577 network.

578 One more seasonality forcing behavior that could be researched is about infodemics.  
579 This was not addressed in this research as a defined region within the time series data, since it  
580 is unpredictable in terms of empirical expression concerning individual and collective behavior  
581 phenomena. In other words, infodemics of subjective reasoning is something that occur  
582 momentarily and independent of time or other static parameters. However it is  
583 predictable when it is adopted by policies as it occurred in some countries. Also it can be  
584 predictable if detected within a community by local authorities.

585

## 586 **5) Conclusion**

587 This research modeled patterns of SARS-COV-2 spreading by redesigning time series  
588 data extraction. This approach opened a new scenario where seasonality forcing behavior was  
589 introduced to understand SARS-COV-2 nonlinear dynamics due to heterogeneity and  
590 confounding scenario of epidemics where actual SIR models might find high degree of  
591 uncertainty. To overcome this limitation it was proposed the division of epidemics curvatures  
592 into regions where compartments of SIR models could be better understood and scientifically  
593 analyzed as well as pointing to the type of seasonality forcing behavior COVID-19 present  
594 worldwide.

595 Regarding curvature features, this research pointed to regions of analysis where  
596 seasonality forcing behavior of SARS-COV-2 finds it is most fitting causality for policies and ALE  
597 interventions, environmental driven factors and urban spaces. These regions were pointed as  
598 the most effective data for monitoring, control and predictive analysis.

599 Concerning the regions of analysis, not only Earth seasons, but atmospheric conditions  
600 (environmental driving seasonality) and urban spaces can present a transmission dynamics  
601 that is hidden in its pattern due to policies/ALE interventions worldwide, thus influencing  
602 predictive analysis of SIR models with uncertainty. However policies and ALE can be the  
603 strongest stable point of seasonality, it can find itself limited at control phase, depending on  
604 the region/country/locality given. This dynamics can be observed briefly, for the moment, in  
605 the random distributions of exponential behavior of countries where outbreaks of first and  
606 second waves are occurring as well as heteroscedasticity form of time series data worldwide.

607 Also, to overcome this hidden patterns scenario, it was found that seasonality forcing  
608 behavior can be tracked by new mathematical tools concerning data extraction among  
609 countries and within countries time period of infection. These tools can reveal new patterns  
610 formation regarding seasonality and therefore contributing to the future use of Fourier  
611 transforms in order to extract periodic phases of SARS-COV-2 transmission under specific set of  
612 parameters. Therefore, following these statements, it is very encouraged that researches in  
613 future adopt this angular momentum (regions of data extraction) of analysis for the  
614 environmental, policies/ALE and urban spaces patterns of transmission.

615

616 **Supplementary Materials:** Some of data used are available at Our World in Data and Outbreak website retrieved  
617 from: <https://outbreak.info/data> and <https://ourworldindata.org>.

618 **Conflicts of Interest:** "The author declares no conflict of interest."

619 **Author Contributions:** Not applicable.

620 **Funding:** "This research received no external funding".

621 **Statement of Ethics:** No humans or animals were involved in this study. Ethics approval was not required.

622 **No trial registration is applied for this study.**

623 **Acknowledgments:** The author feels very grateful for the researchers that made this article possible through  
624 conversations and opinions about policies and ALE, by Henrique Lopes from the Association of Schools of Public  
625 Health in the European Region (ASPHER) and about environmental research by Manuel Hernández Rosales from  
626 Universidad Nacional Autónoma de México.

627

## 628 **References**

- 629 1. Grassly NC, Fraser C. Seasonal infectious disease epidemiology. *Proceedings of the Royal Society B:*  
630 *Biological Sciences.* 2006 Oct 7;273(1600):2541-50.
- 631 2. Su D, Chen Y, He K, Zhang T, Tan M, Zhang Y, Zhang X. Influence of socio-ecological factors on COVID-  
632 19 risk: a cross-sectional study based on 178 countries/regions worldwide. *Regions Worldwide*  
633 (4/17/2020). 2020 Apr 17.
- 634 3. Telles, C. R. (2020). Influence of countries adopted policies for COVID-19 reduction under the view of  
635 the airborne transmission framework. medRxiv.
- 636 4. Block P, Hoffman M, Raabe IJ, Dowd JB, Rahal C, Kashyap R, Mills MC. Social network-based  
637 distancing strategies to flatten the COVID-19 curve in a post-lockdown world. *Nature Human*  
638 *Behaviour.* 2020 Jun 4:1-9.
- 639 5. Ferguson N, Laydon D, Nedjati Gilani G, Imai N, Ainslie K, Baguelin M, Bhatia S, Boonyasiri A,  
640 Cucunuba Perez ZU, Cuomo-Dannenburg G, Dighe A. Report 9: Impact of non-pharmaceutical  
641 interventions (NPIs) to reduce COVID19 mortality and healthcare demand.
- 642 6. Chu DK, Akl EA, Duda S, Solo K, Yaacoub S, Schünemann HJ, El-harakeh A, Bognanni A, Lotfi T, Loeb  
643 M, Hajizadeh A. Physical distancing, face masks, and eye protection to prevent person-to-person  
644 transmission of SARS-CoV-2 and COVID-19: a systematic review and meta-analysis. *The Lancet.* 2020  
645 Jun 1.
- 646 7. Lopes H, McKay V. Adult learning and education as a tool to contain pandemics: The COVID-19  
647 experience. *International Review of Education.* 2020 Jun 18:1-28.

- 648 8. Adam D. Special report: The simulations driving the world's response to COVID-19. *Nature*. 2020  
649 Apr;580(7803):316.
- 650 9. Roberts M, Andreasen V, Lloyd A, Pellis L. Nine challenges for deterministic epidemic models.  
651 *Epidemics*. 2015 Mar 1;10:49-53.
- 652 10. Dong E, Du H, Gardner L. An interactive web-based dashboard to track COVID-19 in real time. *The*  
653 *Lancet infectious diseases*. 2020 May 1;20(5):533-4.
- 654 11. Altizer S, Dobson A, Hosseini P, Hudson P, Pascual M, Rohani P. Seasonality and the dynamics of  
655 infectious diseases. *Ecology letters*. 2006 Apr;9(4):467-84.
- 656 12. Bacaër N. On the biological interpretation of a definition for the parameter  $R_0$  in periodic population  
657 models. *Journal of mathematical biology*. 2012 Oct 1;65(4):601-21.
- 658 13. Siettos CI, Russo L. Mathematical modeling of infectious disease dynamics. *Virulence*. 2013 May  
659 15;4(4):295-306.
- 660 14. Mari L, Casagrandi R, Bertuzzo E, Rinaldo A, Gatto M. Floquet theory for seasonal environmental  
661 forcing of spatially explicit waterborne epidemics. *Theoretical Ecology*. 2014 Nov 1;7(4):351-65.
- 662 15. Zhang Y, You C, Cai Z, Sun J, Hu W, Zhou XH. Prediction of the COVID-19 outbreak based on a realistic  
663 stochastic model. *medRxiv*. 2020 Jan 1.
- 664 16. Utsunomiya YT, Utsunomiya AT, Torrecilha RB, Paulan SD, Milanesi M, Garcia JF. Growth rate and  
665 acceleration analysis of the COVID-19 pandemic reveals the effect of public health measures in real  
666 time. *Frontiers in Medicine*. 2020 May 22;7:247.
- 667 17. Stübinger J, Schneider L. Epidemiology of coronavirus COVID-19: Forecasting the future incidence in  
668 different countries. In *Healthcare 2020 Jun (Vol. 8, No. 2, p. 99)*. Multidisciplinary Digital Publishing  
669 Institute.
- 670 18. Rock K, Brand S, Moir J, Keeling MJ. Dynamics of infectious diseases. *Rep. Prog. Prog.*  
671 *Phys*. 2014;77:026602.
- 672 19. Billings L, Schwartz IB. Exciting chaos with noise: unexpected dynamics in epidemic outbreaks.  
673 *Journal of mathematical biology*. 2002 Jan 1;44(1):31-48.
- 674 20. WHO. World Health Organization: Influenza Laboratory Surveillance Information by the Global  
675 Influenza Surveillance and Response System (GISRS). Generated on 25/06/2020 13:18:33 UTC from:  
676 [https://www.who.int/influenza/gisrs\\_laboratory/flunet/charts/en/](https://www.who.int/influenza/gisrs_laboratory/flunet/charts/en/).
- 677 21. Grenfell BT, Kleczkowski A, Gilligan CA, Bolker BM. Spatial heterogeneity, nonlinear dynamics and  
678 chaos in infectious diseases. *Statistical Methods in Medical Research*. 1995 Jun;4(2):160-83.
- 679 22. Buonomo B, Chitnis N, d'Onofrio A (2018) Seasonality in epidemic models: a literature review.  
680 *Ricerche Mat* 67:7–25
- 681 23. Telles CR. Reducing SARS-CoV-2 infectious spreading patterns by removing S and R compartments  
682 from SIR model equation. *medRxiv*. 2020 Jan 1.
- 683 24. Manzo G. Complex Social Networks are Missing in the Dominant COVID-19 Epidemic Models.  
684 *Sociologica*. 2020 May 20;14(1):31-49.
- 685 25. Merchant H. CoViD-19 may not end as predicted by the SIR model. *The BMJ*. 2020 May  
686 2;369:m1567-rr.
- 687 26. Adam, D. The Simulations Driving the World's Response to COVID-19. How Epidemiologists Rushed  
688 to Model the Coronavirus Pandemic. *Nature*, 580, 316–318. <https://doi.org/10.1038/d41586-020-01003-6>. 2020.
- 689
- 690 27. Luo J. Predictive Monitoring of COVID-19. SUTD Data-Driven Innovation Lab. 2020.
- 691 28. Best R, Boice J. Where The Latest COVID-19 Models Think We're Headed — And Why They Disagree.  
692 *Abc News: FiveThirtyEight*. Retrieved from: <https://projects.fivethirtyeight.com/covid-forecasts/>.  
693 2020 Jun 11.
- 694 29. Koerth M, Bronner L, Mithani J. Why It's So Freaking Hard To Make A Good COVID-19 Model. *Abc*  
695 *News: FiveThirtyEight*. Retrieved from: [https://fivethirtyeight.com/features/why-its-so-freaking-](https://fivethirtyeight.com/features/why-its-so-freaking-hard-to-make-a-good-covid-19-model/)  
696 [hard-to-make-a-good-covid-19-model/](https://fivethirtyeight.com/features/why-its-so-freaking-hard-to-make-a-good-covid-19-model/). 2020 Mar 31.



- 697 30. Liu Y, Ning Z, Chen Y, Guo M, Liu Y, Gali NK, Sun L, Duan Y, Cai J, Westerdahl D, Liu X. Aerodynamic  
698 analysis of SARS-CoV-2 in two Wuhan hospitals. *Nature*. 2020 Apr 27:1-6.
- 699 31. Lin K, Marr LC. Humidity-dependent decay of viruses, but not bacteria, in aerosols and droplets  
700 follows disinfection kinetics. *Environmental Science & Technology*. 2019 Dec 30;54(2):1024-32.
- 701 32. Lidia Morawska, Donald K Milton, It is Time to Address Airborne Transmission of COVID-19, *Clinical*  
702 *Infectious Diseases*, , ciaa939, <https://doi.org/10.1093/cid/ciaa939>
- 703 33. Roda WC, Varughese MB, Han D, Li MY. Why is it difficult to accurately predict the COVID-19  
704 epidemic?. *Infectious Disease Modelling*. 2020 Mar 25.
- 705 34. Duarte J, Januário C, Martins N, Rogovchenko S, Rogovchenko Y. Chaos analysis and explicit series  
706 solutions to the seasonally forced SIR epidemic model. *Journal of mathematical biology*. 2019 Jun  
707 1;78(7):2235-58.
- 708 35. Dietz K (1976) The incidence of infectious diseases under the influence of seasonal fluctuations. In:  
709 *Mathematical models in medicine*. Springer, Berlin, pp 1–15
- 710 36. Telles CR. False Asymptotic Instability Behavior at Iterated Functions with Lyapunov Stability in  
711 *Nonlinear Time Series*. arXiv preprint arXiv:1911.07646. 2019 Nov 13.
- 712 37. Jiang R, Murthy DN. A study of Weibull shape parameter: Properties and significance. *Reliability*  
713 *Engineering & System Safety*. 2011 Dec 1;96(12):1619-26.
- 714 38. Edelsbrunner, H., & Harer, J. (2008). Persistent homology-a survey. *Contemporary mathematics*, 453,  
715 257-282.
- 716 39. Cohen-Steiner D, Edelsbrunner H, Harer J. Stability of persistence diagrams. *Discrete &*  
717 *computational geometry*. 2007 Jan 1;37(1):103-20.
- 718 40. CDC. Centers for Disease Control and Prevention. CASES, DATA & SURVEILLANCE: Forecasts of Total  
719 Deaths July 2, 2020. Retrieved at: [https://www.cdc.gov/coronavirus/2019-ncov/covid-](https://www.cdc.gov/coronavirus/2019-ncov/covid-data/forecasting-us.html)  
720 [data/forecasting-us.html](https://www.cdc.gov/coronavirus/2019-ncov/covid-data/forecasting-us.html), on 08 July, 2020.
- 721